Title

Differences in the resting-state fMRI global signal amplitude between the eyes open and eyes closed states are related to changes in EEG vigilance.

Journal

NeuroImage, 124(Pt A)

ISSN

1053-8119

Authors

Wong, Chi Wah
DeYoung, Pamela N
Liu, Thomas T

Publication Date

2016

DOI

10.1016/j.neuroimage.2015.08.053

Peer reviewed

Differences in the resting-state fMRI global signal amplitude between the eyes open and eyes closed states are related to changes in EEG vigilance

Chi Wah Wong[1,2], Pamela N. DeYoung[4,5], and Thomas T. Liu[1,2,3]

[1]Center for Functional Magnetic Resonance Imaging,
Departments of [2]Radiology and [3]Bioengineering,
and [4]Division of Pulmonary and Critical Care Medicine
University of California San Diego, La Jolla, California, USA
[5]Division of Sleep Medicine
Brigham and Women's Hospital and Harvard Medical School, Boston, Massachusetts, USA

Correspondence to:
Chi Wah Wong, Ph.D.
UCSD Center for Functional MRI
9500 Gilman Drive, MC 0677
La Jolla, CA 92093-0677
Phone: 858-822-0513
Fax: 858-822-0605
E-mail: cwwong@ieee.org

Thomas T. Liu, Ph.D.
UCSD Center for Functional MRI
9500 Gilman Drive, MC 0677
La Jolla, CA 92093-0677
Phone: 858-822-0542
Fax: 858-822-0605
E-mail: ttliu@ucsd.edu

Abstract

In resting-state functional connectivity magnetic resonance imaging (fcMRI) studies, measures of functional connectivity are often calculated after the removal of a global mean signal component. While the application of the global signal regression approach has been shown to reduce the influence of physiological artifacts and enhance the detection of functional networks, there is considerable controversy regarding its use as the method can lead to significant bias in the resultant connectivity measures. In addition, evidence from recent studies suggests that the global signal is linked to neural activity and may carry clinically relevant information. For instance, in a prior study we found that the amplitude of the global signal was negatively correlated with EEG measures of vigilance across subjects and experimental runs. Furthermore, caffeine-related decreases in global signal amplitude were associated with increases in EEG vigilance. In this study, we extend the prior work by examining measures of global signal amplitude and EEG vigilance under eyes-closed (EC) and eyes-open (EO) resting-state conditions. We show that changes (EO minus EC) in the global signal amplitude are negatively correlated with the associated changes in EEG vigilance. The slope of this EO-EC relation is comparable with the slope of the previously reported relation between caffeine-related changes in the global signal amplitude and EEG vigilance. Our findings provide further support for a basic relationship between global signal amplitude and EEG vigilance.

Keywords: resting-state fMRI, eyes-open, eyes-closed, global signal, vigilance, electroencephalography

Introduction

In recent years, resting-state functional magnetic resonance imaging (fMRI) has been increasingly used as a tool to study functional brain connectivity in both health and disease (Fox and Raichle, 2007). The functional connectivity measures used in resting-state fMRI reflect the temporal synchrony of blood oxygenation level dependent (BOLD) signals across brain regions (Biswal et al., 1995; Fox et al., 2005; Fransson, 2005; Raichle et al., 2001). These connectivity measures are often dominated by the presence of a global signal component that appears to varying extents across the brain. To deal with this effect, many studies have adopted a pre-processing approach referred to as global signal regression (GSR), in which the global signal component is regressed out of the measured BOLD signals prior to the computation of connectivity measures. This approach has been shown to increase the spatial specificity of the correlation maps and to better reveal the anti-correlation between resting-state networks (e.g. the default mode network and the task positive network) (Birn, 2012; Fox et al., 2005; Greicius et al., 2003). However, there is some concern about the use of GSR, as it has been shown to introduce systematic biases into correlation-based measures of functional connectivity (Fox et al., 2009; Hahamy et al., 2014; Murphy et al., 2009; Saad et al., 2012). At present, there is not a universally agreed upon standard regarding the use of GSR, with some studies employing GSR, other studies using alternate noise reduction methods, and yet another set of studies that perform analyses with and without the use of GSR (Yeo et al., 2015).

In conjunction with the ongoing discussion regarding the use of GSR, there has also been interest in developing a better understanding of the global signal. In a study of resting monkeys, (Scholvinck et al., 2010) reported that the local field potential power measured at a single cortical site exhibited widespread correlation with BOLD fMRI signals, providing evidence of a neural basis for the global signal. A recent study in sleep-deprived monkeys has demonstrated that specific neurophysiological events observed during sleep are associated with large scale fluctuations in cerebral blood volume and may therefore represent significant contribution to the global signal (Liu et al., 2015a; Liu et al., 2015b). Using simultaneous EEG-fMRI measures in human subjects, we have shown that the amplitude of the global signal was inversely

correlated with electroencephalographic (EEG) measures of vigilance across subjects and experimental runs (Wong et al., 2013), with higher vigilance states characterized by lower global signal amplitudes (defined as the standard deviation of the global signal). In addition, we found that increases in EEG vigilance measures associated with the ingestion of caffeine were significantly correlated with decreases in the global signal amplitude. There is also some evidence that the global signal may carry diagnostic information. For example, (Yang et al., 2014) recently reported that the variance of the global signal was significantly lower in patients with schizophrenia as compared to normal controls. However, the authors of that study acknowledged that the potential confound of vigilance differences between groups would need to be carefully considered in follow-up work.

In this study, we extend our prior work to determine whether the previously described relation between the global signal and vigilance would also be observed when contrasting measures obtained in the eyes-open versus eyes-closed states. Prior studies have shown that resting-state fMRI activity is significantly different between the eyes-closed and eyes-open conditions (Bianciardi et al., 2009; Jao et al., 2013; McAvoy et al., 2008; Patriat et al., 2013; Xu et al., 2014; Yan et al., 2009; Yang et al., 2007; Yuan et al., 2014; Zou et al., 2009). In general, these studies have found that the amplitude of the resting-state BOLD signal is decreased in the eyes-open condition as compared to the eyes-closed condition. For example, (Jao et al., 2013) found that the average variance of the BOLD signal (i.e. signal variances computed on a per-voxel basis and then averaged across the brain) was significantly lower in the eyes-open condition. Furthermore, in our earlier studies, we reported that global signal effects were generally lower in the eyes-open condition as compared to the eyes-open condition (Wong et al., 2012, 2013). Taking into account the prior findings, we hypothesized that decreases in global signal amplitude associated with opening of the eyes would be correlated with increases in EEG vigilance measures. We also examined whether the relationship between changes in the global signal amplitude and vigilance observed with the opening of the eyes would be similar to the relationship previously observed with the administration of caffeine (Wong et al., 2013).

Methods

Experimental protocol

Twelve healthy volunteers were initially enrolled in this study after providing informed consent. Two subjects were not able to complete the entire study, resulting in a final sample size of 10 subjects (4 males and 6 females, aged 24 to 33 years with an average age of 25.6 years). As prior work has shown that differences in dietary caffeine consumption may cause variability in the BOLD response (Laurienti et al., 2002), we recruited caffeine-naive subjects who consumed less than 50 mg caffeine daily (as assessed over a two month period prior to the study).

In this study we used data from the protocol described in our prior work (Wong et al., 2012, 2013). A repeated measures design was used, with each subject participating in two imaging sessions: a caffeine session and a control session. For the test of the primary hypotheses in this study, we analyzed the eyes-open and eyes-closed data from the control session. For the additional analysis, we compared the current findings with our prior analysis of the eyes-closed data from the caffeine session (Wong et al. 2013).

The order of the two sessions was randomized in a double-blinded manner. For each session, the operator obtained a capsule that contained 200 mg of either caffeine or cornstarch. The two imaging sessions were separated by at least two weeks. Each session consisted of a pre-dose and a post-dose imaging section, with each section lasting for about one hour. Upon completion of the pre-dose section, participants were taken out of the magnet and given the capsule. The subject was then placed back in the scanner, with the first functional scan of the post-dose section obtained approximately 40 minutes after capsule ingestion. This interval was chosen based on studies showing that the absorption of caffeine from the gastrointestinal tract reaches 99% about 45 min after ingestion, with a half-life ranging from 2.5 to 4.5 hours (Fredholm et al., 1999).

Each scan section consisted of (1) a high-resolution anatomical scan, (2) arterial spin labeling scans (these results are reported in our prior study (Wong et al., 2012) but not

considered here), and (3) two 5 minute resting-state scans with simultaneous EEG recording (one eyes-closed and one eyes-open). Subjects were instructed to lie still in the scanner and not fall asleep during resting-state scans. The order of the eyes-open and eyes-closed scans was randomized. During the eyes-open (EO) resting-state scans, subjects were asked to maintain attention on a black square located at the center of a gray background. During the eyes-closed (EC) resting-state scans, subjects were asked to imagine the black square. An impedance check was performed prior to each EEG data acquisition while the subject was in the desired state (EC or EO) for at least 1.5 minutes. EEG data acquisition began 30 seconds before each fMRI scan and ended 30 seconds after. Thus, the subject was in the desired state (EC or EO) for at least 2 minutes prior to the acquisition of the combined EEG and fMRI data. Field maps were acquired to correct for magnetic field inhomogeneities.

MR Data acquisition

Imaging data were acquired on a 3 Tesla GE Discovery MR750 whole body system using an eight-channel receiver coil. High resolution anatomical data were collected using a magnetization prepared 3D fast spoiled gradient (FSPGR) sequence (TI=600 ms, TE=3.1 ms, flip angle = 8 degrees, slice thickness = 1 mm, FOV = 25.6 cm, matrix size = 256x256x176).

Whole brain BOLD resting-state data were acquired over thirty axial slices using an echo planar imaging (EPI) sequence (flip angle = 70 degrees, slice thickness = 4 mm, slice gap = 1 mm, FOV = 24 cm, TE = 30 ms, TR = 1.8 s, matrix size = 64x64x30).

Field maps were acquired using a gradient recalled acquisition in steady state (GRASS) sequence (TE1 = 6.5 ms, TE2 = 8.5 ms), with the same in-plane parameters and slice coverage as the BOLD resting-state scans. The phase difference between the two echoes was then used for magnetic field inhomogeneity correction of the BOLD data.

Cardiac pulse and respiratory effect data were monitored using a pulse oximeter (InVivo) and a respiratory effort transducer (BIOPAC), respectively. The pulse oximeter was placed on each subject's right index finger while the respiratory effort belt was placed around each

subject's abdomen. Physiological data were sampled at 40 Hz using a multi-channel data acquisition board (National Instruments).

EEG Data acquisition

EEG data were recorded using a 64 channel MR-compatible EEG system (Brain Products, Munich, Germany). The system consisted of two 32 channel BrainAmp MR Plus amplifiers powered by a rechargeable battery unit. The system was placed behind the scanner bore, which was connected using a 125 cm long data cable to a BrainCap MR with 64 recording electrodes (Brain Products, Munich, Germany). All electrodes in the cap had sintered Ag/AgCl sensors incorporating 5 kΩ safety resistors. The separate ECG electrode had a built-in 15 kΩ resistor. The arrangement of the electrodes in the cap conformed to the international 10/20 standard. FCz and AFz were the reference and ground electrodes, respectively. The EEG data were recorded at a 5 kHz sampling rate with a passband of 0.1-250 Hz. A phase locking device (Syncbox, Brain Products, Munich, Germany) was used to synchronize the clock of the EEG system with the master clock of the MRI system. Before each scan section, the electrode impedances were set below 20 kΩ, while the impedances of the reference and ground electrodes were set below 10 kΩ. Prior to recording EEG data in each resting-state scan, a snapshot of the electrode impedance values was taken from the computer screen. One EEG dataset was created for each 5-min resting-state scan.

MR data pre-processing

Details of MR and EEG data pre-processing were described in our prior article (Wong et al., 2013) and are repeated here for the reader's convenience. AFNI and FSL were used for MRI data pre-processing (Cox, 1996; Smith et al., 2004; Woolrich et al., 2009). The high resolution anatomical data were skull stripped and segmentation was applied to estimate white matter (WM), gray matter (GM) and cerebral spinal fluid (CSF) partial volume fractions. In each scan section, the anatomical volume was aligned to the middle functional volume of the first resting-state run using AFNI. The anatomical volume in the post-dose scan section was then registered

to the pre-dose anatomical volume, and the rotation and shift parameters obtained from this registration were applied to the post-dose functional images.

The first 6 TRs (10.8 seconds) of the BOLD data were discarded to allow magnetization to reach a steady state. A binary brain mask was created using the skull-stripped anatomical data. For each slice, the mask was eroded by two voxels along the border to eliminate voxels at the edge of the brain (Rack-Gomer and Liu, 2012). For each run, nuisance terms were removed from the resting-state BOLD time series through multiple linear regression. These nuisance regressors included: i) linear and quadratic trends, ii) six motion parameters estimated during image co-registration and their first derivatives, iii) RETROICOR (2^{nd} order Fourier series) (Glover et al., 2000) and RVHRCOR (Chang and Glover, 2009) physiological noise terms calculated from the cardiac and respiratory signals, and iv) the mean BOLD signals calculated from WM and CSF regions and their first respective derivatives, where these regions were defined using partial volume thresholds of 0.99 for each tissue type and morphological erosion of two voxels in each direction to minimize the inclusion of gray matter. We assessed the amount of head motion for each subject by first calculating the framewise displacement (FD) as defined by (Power et al., 2012) using the 6 motion parameter time courses. An average measure of head motion was then obtained by averaging the FD across time.

EEG data pre-processing

Vision Analyzer 2.0.1 software (Brain Products, Munich, Germany) was used for MR gradient removal using an average pulse artifact template procedure (Allen et al., 2000). An average template was created using the volume-start markers from the MRI system and then subtracted from the individual artifacts. After gradient artifact removal, a low pass filter with a cutoff frequency of 30 Hz was applied to all channels and the processed signals were down-sampled to 250 Hz. Heart beat event markers were created within the Analyzer software. The corrected data and event markers were exported to MATLAB (Mathworks, Inc.).

EEGLAB (version 9) was used for further pre-processing (Delorme and Makeig, 2004). For each EEG dataset, the ballistocardiogram (BCG) and residual artifacts were removed using a

combined optimal basis set and independent component analysis approach (OBS-ICA) (Debener et al., 2007; Niazy et al., 2005). To remove the BCG artifact, the continuous EEG data were divided into epochs based on the heart beat event markers. The epochs were stacked into a matrix configuration and a BCG template was created using the first three principal components calculated from the matrix (Debener et al., 2007). The BCG template was then fitted in a least-squares manner and subtracted from each epoch of the EEG data.

After BCG artifact removal, channels that exhibited high impedance values (>20 kΩ) or were contaminated with high levels of residual gradient artifact were identified and discarded from further processing. The impedance values were identified using the snapshot of channel impedances acquired before the beginning of each scan. To identify channels contaminated with residual gradient artifact that was not adequately removed using the Analyzer software, the continuous EEG data in each channel were bandpass filtered from 15.5 to 17.5 Hz. This frequency band contained the first harmonic of the gradient artifact centered at 16.7 Hz (slice markers were separated by 60 ms). The root mean square (rms) of the filtered time course was calculated for each channel. A channel was identified as a contaminated channel if the rms value was larger than the median plus 6 times the inter-quartile range (Devore and Farnum, 2005), calculated across all channels except the ECG. On average, each channel was included in 95% of the runs in both the eyes-closed and eyes-open conditions (median=98%, s.d.=6%). For further analysis, only the included channels for each run were used.

Extended infomax ICA was then performed. Independent Components (ICs) corresponding to residual BCG or eye blinking artifacts were identified by correlating all IC topographies with artifact template topographies and extracting the ICs with spatial correlation values of 0.8 or more (Debener et al., 2007; Viola et al., 2009). The corrected data were then created by projecting out the artifactual ICs (Delorme and Makeig, 2004).

Manual sleep staging was performed by a registered polysomnographic technologist using AASM guidelines (AASM, 2009). Specifically, the corrected data (using channels F3, F4, C3, C4, O1 and O2) were segmented into 30 second epochs (with 10 epochs per run) and a sleep stage was scored for each epoch. Based on the sleep staging, it was determined that one subject was not awake during the majority of their scans, and this subject was excluded from further

analysis. All of the remaining nine subjects were awake during all 20 epochs of the eyes-open runs. For the eyes-closed runs, five subjects were awake during all 20 epochs. The remaining 4 subjects were awake during the majority of the epochs, but had some epochs with stage N1, with two subjects also exhibiting one or two epochs of stage N2. Table 1 indicates the number of epochs observed for each sleep stage during the eyes-closed scans, as well as the number of vertex sharp waves and K-complex events.

As bulk head motion creates high amplitude distortion in the EEG data acquired in the MRI environment, it is desirable to discard the distorted time segments (Jansen et al., 2012; Laufs et al., 2008). To identify the contaminated time segments, the EEG data were bandpass filtered from 1 to 15 Hz (to avoid the first harmonic of the residual gradient artifact centered at 16.7 Hz). A mean amplitude time series was calculated by taking the rms across channels. Outlier detection was performed on the mean time series and the outlier threshold was calculated as the sum of the median value and 6 times the inter-quartile range across time (Devore and Farnum, 2005). Data points with values larger than this threshold were regarded as segments contaminated by motion. Contaminated segments less than 5 seconds apart were merged to form larger segments that were then excluded. A binary time series was created by assigning a "1" to the time points within the bad time segments and a "0" to remaining good time points.

In a recent study, (Jansen et al., 2012) found that predictors derived from EEG motion artifact were strongly correlated with the BOLD signal when the EEG predictors were convolved with a hemodynamic response function. To indicate the time points reflecting the BOLD response to the motion artifact, we convolved the binary time series with a hemodynamic response function (Buxton et al., 2004) and binarized the resulting output with a threshold of zero to form a second binary time series. Since both EEG and fMRI measures were considered in our study, a final binary time series was created by combining the two binary time series using an OR operation. The binary time series were down-sampled to match the sampling frequency of the BOLD time courses. In the eyes-closed condition, an average of 81% of the time points of the binary time series were indicated as good (i.e. with a value of zero; median=85%, s.d.=13%). In the eyes-open condition, the corresponding average was 86% (median=88%, s.d.=9%). The application of the binary time series is described in the next paragraph.

For each EEG channel, a spectrogram was created using a short-time Fourier transform with 4-term Blackman-Harris window (1311 points, 5.24 s temporal width, and 65.7% overlap). The output temporal resolution of the spectrogram was 1.8s (i.e. equivalent to the TR of the BOLD resting-state scans). The time points in the EEG spectrogram and BOLD time series that were indicated as potentially contaminated by motion (i.e. values of 1 in the binary time series) were discarded from further analysis.

Calculating the fMRI and EEG metrics

For each voxel, a percent change time series was obtained from the pre-processed BOLD time series by subtracting the mean value and then dividing the resulting difference by the mean value. A global mean signal was formed as the average of the percent change time series across all voxels within the brain, and the global signal amplitude was defined as the standard deviation of this mean signal for data from the pre-dose and post-dose control sessions.

As described above, a spectrogram was calculated for each EEG channel with the same temporal resolution as the BOLD time series, and potentially motion-contaminated time points in the spectrogram were removed. For each remaining time point in the spectrogram, a relative amplitude spectrum was computed by normalizing the spectrum by its overall rms amplitude (square root of sum of squares across all frequency bins). A global relative amplitude spectrum was created by taking the rms of all spectra across channels and time points in the control sessions. Relative EEG amplitudes were then computed as the rms amplitude in the following frequency bands (delta: 1-4 Hz, theta: 4-7 Hz, alpha: 7-13 Hz, beta: 13-30 Hz). A measure of vigilance was defined as the rms amplitude in the alpha band divided by the rms amplitude in the delta and theta bands (Horovitz et al., 2008; Olbrich et al., 2009), which is equivalent to the alpha slow-wave index (ASI) (Jobert et al., 1994; Larson-Prior et al., 2009; Muller et al., 2006).

Changes (EO-EC) in global signal amplitude and vigilance were computed and the relationship between these changes was assessed with a linear regression model. In addition, we compared the current findings with the relationship previously reported for changes in

global signal amplitude and vigilance due to the administration of caffeine (Wong et al., 2013). The data from the present (EO-EC) and prior (post-dose caffeine minus pre-dose) studies were analyzed together using a general linear model consisting of the change in global signal amplitude as the dependent variable and the following independent variables: an overall mean term, a group indicator term (e.g. EO-EC or post-pre caffeine), the change in vigilance for the EO-EC data, and the change in vigilance for the caffeine post-pre data. A F-test was used to compare the slopes estimated for the relations between global signal amplitude and vigilance for the EO-EC and caffeine post-pre data.

To assess the robustness of the findings, we repeated the analysis process with various modifications as follows First, to delineate the potential impact of periods of sleep on the findings (Horovitz et al., 2008; Tagliazucchi et al., 2013), we computed two additional versions of the metrics, in which we limited the analysis of the data to include either (1) only Wake or N1 epochs or (2) only Wake epochs. In addition, for the data restricted to either only Wake or N1 epochs, we computed an third version in which data segments within the N1 epochs that exhibited vertex sharp waves were excluded from the analysis, as these events have been shown to influence the fMRI signal (Caporro et al., 2012; Jahnke et al., 2012; Stern et al., 2011). Second, we computed three additional versions of the metrics in which the calculation was restricted to gray matter, white matter, or cerebrospinal fluid voxel, with a partial volume threshold of 0.99 for each tissue type. Third, we also recomputed the metrics after excluding voxels in which high variance voxels (top 2% of variance) were excluded from the computation of the global signal (Behzadi et al., 2007). Finally, we considered the relation between the changes in global signal amplitude and changes in motion (calculated as the FD parameter described above), mean respiration rate, and mean heart rate, where the latter two metrics were as computed as the inverse of the mean interval between consecutive peaks in the respiration data and EEG heart beat event markers (Olbrich et al., 2009), respectively.

Results

In Fig. 1a, we show the relation between the changes (EO-EC) in the global signal amplitudes and the respective changes in EEG vigilance across all epochs that included primarily awake states (84% of all EC epochs) with some epochs of stage N1 and N2 (14.4% and 1.6% of all EC epochs, respectively). Note that all EO epochs were assessed to be in the Wake stage. There was a significant negative correlation ($r=-0.84$; $p=0.005$) between the changes in global signal amplitude and EEG vigilance. This negative correlation persisted even when considering EC data from (1) only Wake or N1 epochs (Fig. 1b; $r=-0.8$, $p = 0.009$); (2) only Wake or N1 epochs with exclusion of data segments surrounding vertex sharp waves in the N1 epochs (Fig. 1c; $r = -0.8$; $p = 0.01$); and (3) only Wake epochs (Fig. 1d; $r = -0.78$; $p = 0.01$).

Example amplitude spectra from two representative subjects are shown in Figs. 2b and 2c, with the plot from Fig. 1a shown again as Fig. 2a to facilitate comparison of the data. In Fig. 2b, there is relatively little change in the spectra between the EC and EO conditions, corresponding to a relatively small change in both the global signal amplitude and vigilance measures. In contrast, the spectra in Fig. 2c shows a pronounced shift towards higher frequencies in the EO condition as compared to EC, corresponding to a large increase in vigilance and a large decrease in the global signal amplitude.

The robustness of the relationships reported in Fig. 1 was examined using various modifications of the analysis. When excluding voxels with high signal variance, a significant negative correlation ($p < 0.02$) between changes in global signal amplitude and vigilance was still found for each of the 4 conditions described above for Fig. 1, with the correlation values ranging from $r = -0.75$ to -0.83. This partly reflects the fact that in the primary analysis we had already eroded two voxels at the brain edges to minimize the presence of high-variance edge voxels. Restriction to gray matter voxels resulted in a similar range of correlation values ($r = -0.77$ to -0.80), with all relations remaining significant ($p < 0.02$). No significant relation was found when restricting voxels to white matter ($r = -0.05$ to 0.10; $p > 0.79$). For voxels in cerebral spinal fluid, the relationship was not significant when using data that included N1 and N2 epochs ($r = -0.46$ to -0.51; $p > 0.16$) and was nearly significant when only Wake epochs were

used ($r = -0.64$; $p = 0.06$), most likely reflecting some degree of residual partial voluming with gray matter. In addition, we considered the relation between changes in global signal amplitude and vigilance across the two EO control sessions, and did not find a significant correlation ($r = -0.21$; $p = 0.6$). This may partly reflect the fact that the spread of the changes in both the global signal amplitude and vigilance across the EO sessions was roughly half that observed in the comparison of EO versus EC sessions (in Figure 1). To be specific, for the vigilance changes, the standard deviation of the EO-EC changes was 1.7 to 1.8 times larger (across the different processing options shown in Figure 1) than that observed across the EO sessions, while the mean absolute deviation was 2.2 to 2.3 times larger. Similarly, for the changes in global signal amplitude, the standard deviation of the EO-EC changes was 1.8 to 2.0 times larger and the mean absolute deviation was 2.1 to 2.3 times larger than the respective changes across EO sessions.

We also investigated the relation between the changes in global signal amplitude and the physiological and motion metrics. We did not find a significant correlation between changes in global signal amplitudes and either changes in average FD ($r = 0.23$ to 0.46; $p > 0.22$) or respiration rate ($r = -0.30$ to -0.37; $p > 0.33$). There was a significant negative correlation between changes in global signal amplitude and changes in the mean heart rate ($r = -0.69$ to -0.71; $p < 0.04$) when all epochs, only Wake and N1 epochs, or Wake and N1 epochs (with vertex sharp waves removed) were included in the analysis, but this relation did not reach significance ($r = -0.58$; $p = 0.10$) when considering only the Wake epochs. This finding was consistent with a significant ($r = 0.68$ to 0.73; $p < 0.045$) positive correlation between changes in EEG vigilance and the mean heart rate and with prior findings showing a correlation between vigilance and heart rate (Olbrich et al., 2011).

In Fig. 3, we examine whether the relationship between changes in the global signal amplitude and vigilance observed with the opening of the eyes is similar to the relationship previously observed with the administration of caffeine (Wong et al., 2013). As in Fig. 1, the subplots show the results obtained with the different analysis options. Differences (EO-EC) in global signal amplitude versus differences in vigilance from Fig. 1 are plotted in blue, while the caffeine-related differences (post-dose minus pre-dose) in these metrics that were previously

examined in (Wong et al., 2013) are plotted in red. The blue and red dashed lines indicate the linear fits to the EO-EC and caffeine data, respectively. As shown in Fig. 3a, when data from all epochs are used, both datasets exhibit a negative slope, with a slightly steeper slope for the ECEO data, although the difference in slopes was not significant ($F(1,14) = 3$, $p = 0.1$). When restricting the data used to 1) only Wake or N1 epochs (Fig. 3b); (2) only Wake or N1 epochs with exclusion of data segments surrounding vertex sharp waves in the N1 epochs (Fig. 3c); or (3) only Wake epochs (Fig. 3d), the ECEO and caffeine data showed similar negative slopes, with no significant differences found in the slopes ($F(1,14) < 2.1$; $p > 0.17$).

Discussion

We have shown that changes in the global signal amplitude (EO-EC) are negatively correlated with the associated changes in EEG vigilance measures. The slope of the relationship obtained with EO-EC changes was comparable to the slope of the previously reported relationship between caffeine-related changes in the global signal amplitude and EEG vigilance (as measured in the EC condition). These findings were robust with respect to variations in the analysis procedure. In particular, as a recent study has shown a reliable loss of wakefulness in resting-state studies (Tagliazucchi and Laufs, 2014), we analyzed the data using a range of inclusion criteria for data epochs based on sleep staging. We found that the relationship between changes in global signal and EEG vigilance was evident whether all epochs (including those with N1 and N2 sleep) were used or when a restricted set of epochs (e.g. only Wake epochs) were considered. This finding suggests that the observed relationship may hold across a range of sleep stages, consistent with the prior findings discussed below. However, given the limited number of N1 and N2 epochs (0% of the total number of EO epochs and 16% of the total number of EC epochs) observed in this study, further studies with a greater fraction of sleep epochs would be needed to fully test this conjecture. For example, studies in sleep deprived subjects would be useful in this respect (Ong et al., 2015; Yeo et al., 2015).

Although the origins and interpretation of the global signal are still not well delineated, the results of the current study add to the body of prior findings indicating that the global signal contains a significant neural component (Liu et al., 2015a; Liu et al., 2015b; Scholvinck et al.,

2010; Wong et al., 2013). In our prior study, we reported an inverse correlation between global signal amplitude and EEG vigilance as observed across subjects and experimental runs, and furthermore showed that caffeine-related decreases in global signal amplitude were associated with increases in vigilance (Wong et al., 2013). In related studies, the BOLD signal amplitude has been found to increase as subjects enter into light sleep stages and exhibit lower levels of vigilance (Fukunaga et al., 2006; Horovitz et al., 2008; Larson-Prior et al., 2009; Olbrich et al., 2009). Our current finding of a relation between the decrease in global signal amplitude and increase in vigilance (observed with the change from the EC to EO state) is consistent with these prior findings and provides further evidence for a general relationship between global signal amplitude and vigilance. Indeed, the similarity between the relationships observed for the EO-EC changes and the caffeine-related changes suggest that the basic components of this relationship are to some extent independent of the experimental manipulation. Further work is needed to better understand the mechanisms relating vigilance and global signal amplitude, including the extent to which the underlying sources vary across levels of wakefulness and sleep.

Prior studies have generally found that resting-state BOLD activity is reduced in the EO state as compared to the EC state (Bianciardi et al., 2009; Jao et al., 2013; McAvoy et al., 2008; Patriat et al., 2013; Xu et al., 2014; Yan et al., 2009; Yang et al., 2007; Yuan et al., 2014; Zou et al., 2009). While there is some diversity in the findings, with regional resting-state activity sometimes found to be higher in the EO condition, it is likely that these differences reflect variations in processing approaches, such as the use of global signal regression and physiological noise reduction in some studies and not others. Decreases in functional connectivity in the EO state as compared to the EC state have also been reported (Bianciardi et al., 2009; Xu et al., 2014; Zou et al., 2009), and are consistent with a decrease in global signal. Our findings suggest that changes in both global signal amplitude and EEG vigilance should be considered in the interpretation of studies that examine differences in resting-state activity between the EC and EO states. For example, decreases in global signal amplitude and increases in vigilance may account for the increased reliability of connectivity measure obtained in the EO condition as compared to the EC state (Patriat et al., 2013).

With respect to the EEG vigilance measures, it should be noted that the measures were obtained from 5-minute long scans in which the subject was in the desired state (i.e. EC or EO) for at least two minutes prior to the start of the 5-minute acquisition period. This is consistent with the approach of prior resting-state fMRI studies in which subjects are usually measured in an EC or EO state lasting for 5 minutes or more. In contrast, EEG experiments typically have subjects open and close their eyes in alternating short intervals (e.g. 2 minutes EC followed by 2 minutes EO) (Barry et al., 2011; Barry et al., 2007; Michels et al., 2013). Such alternating paradigms are more likely to elicit Berger's effect in which the alpha rhythm becomes blocked by opening of the eyes. However, the blockage can be limited to a few seconds in some subjects and alpha rhythms typically reappear within a few minutes of opening of the eyes (Neidermeyer, 1999). Given the longer paradigms used in this study, the presence of this blockage in the EO state was likely to have had a minimal influence on the vigilance measures.

Similar to the experimental protocols used in the vast majority of resting-state fMRI studies and prior studies specifically examining the contrast between eyes open and eye closed conditions (Bianciardi et al., 2009; Jao et al., 2013; McAvoy et al., 2008; Patriat et al., 2013; Xu et al., 2014; Yan et al., 2009; Yang et al., 2007; Yuan et al., 2014; Zou et al., 2009), subjects were instructed to keep their eyes open (with fixation) or eyes closed but there was not an explicit measurement of the state of the eyes. Compliance with the instructions may be partially inferred from the lack of sleep in the EO condition. Nevertheless, given the relationship shown here between changes in vigilance and global signal and the findings of (Tagliazucchi and Laufs, 2014) showing that wakefulness in resting-state fMRI is more likely when subjects are instructed to keep their eyes open, future resting-state fMRI studies may need to consider monitoring of the eye states, especially in populations where compliance with instructions may not be high.

In this paper, we have followed the nomenclature employed by prior studies (Jobert et al., 1994; Matejcek, 1982; Olbrich et al., 2009) in our use of the term vigilance. For example, Jobert et al (1994) referred to the use of the alpha slow-wave index (which is identical to the vigilance metric used in this paper) as "a descriptor of the state of vigilance." Related terms such as "EEG

arousal index," "cortical arousal," "wakefulness," or "alertness" are also applicable and have been used in a number of influential prior studies (Olbrich et al., 2011; Sadaghiani et al., 2010).

In conclusion, our observation of a relationship between changes in the global signal amplitude and EEG vigilance across the EC and EO states extends the prior findings, providing further evidence for a substantial neural contribution to the global signal. In addition, the similarity of the slope of the relationship to that previously found with the administration of caffeine suggests the existence of a common mechanism governing the link between the global signal and EEG vigilance. It will be important for investigators to keep this link in mind when interpreting resting-state data, especially when there may be systematic differences in vigilance across groups or conditions.

Acknowledgements

This work was supported in part by NIH Grants R01NS051661 and R21MH096495, and ONR MURI Award No. N00014-10-1-0072.

Table 1: For each subject, the number of epochs (maximum of 20) in the Wake, N1, and N2 sleep stages for the eyes-closed data sets are listed. The numbers of vertex sharp waves and k-complex events are also provided. Note that for the eyes-open data sets, all epochs were found to be in the Wake stage.

Subject	Wake	N1	N2	Number of vertex sharp waves	Number of k-complexes
1	20	0	0	0	0
2	14	6	0	8	0
3	20	0	0	0	0
4	13	7	0	2	0
5	13	5	2	0	2
6	20	0	0	0	0
7	20	0	0	0	0
8	20	0	0	0	0
9	11	8	1	2	1
Total	151	26	3	12	3

Figure Captions

Figure 1. Plots showing a significant negative correlation between changes (EO-EC) in global signal amplitude (y-axis) and in EEG vigilance (x-axis). The results shown represent processing of data from (a) all epochs, (b) only Wake or N1 epochs; (c) only Wake or N1 epochs with exclusion of data segments surrounding vertex sharp waves in the N1 epochs, and (d) only Wake epochs.

Figure 2. The EEG spectra for two representative subjects are shown in panels b and c, alongside the plot (panel a) of changes in global signal amplitude versus EEG vigilance previously presented in Figure 1a. The EO and EC states are indicated by the cyan and brown lines, respectively. When there is relatively little difference between the EO and EC spectra (panel b), there are minimal changes in both the global signal amplitude and EEG vigilance. When there is a pronounced shift to higher frequencies in the EO spectrum (panel c), there is a sizeable decrease in the global signal amplitude accompanied by a substantial increase in vigilance.

Figure 3. Comparisons of the relation between global signal amplitude and EEG vigilance associated with changes due to either opening of the eyes or administration of caffeine. The changes (EO-EC) in the average global signal amplitude versus associated differences in EEG vigilance are indicated by the blue symbols with the linear fit shown by the blue dashed line. Changes (post-dose caffeine minus pre-dose) in the global signal amplitude versus the associated changes in EEG vigilance from (Wong et al., 2013) are indicated by the red symbols with the linear fit shown by the red dashed line. The solid grey line shows the overall linear fit to all the data points. The results shown represent processing of data from (a) all epochs, (b) only Wake or N1 epochs; (c) only Wake or N1 epochs with exclusion of data segments surrounding vertex sharp waves in the N1 epochs, and (d) only Wake epochs. For all processing options, there was not a significant difference in the slopes of the two dashed lines.

References

AASM, 2009. The AASM Manual for the Scoring of Sleep and Associated Events: Rules, Terminology and Technical Specification.

Allen, P.J., Josephs, O., Turner, R., 2000. A method for removing imaging artifact from continuous EEG recorded during functional MRI. NeuroImage 12, 230-239.

Barry, R.J., Clarke, A.R., Johnstone, S.J., 2011. Caffeine and opening the eyes have additive effects on resting arousal measures. Clin Neurophysiol 122, 2010-2015.

Barry, R.J., Clarke, A.R., Johnstone, S.J., Magee, C.A., Rushby, J.A., 2007. EEG differences between eyes-closed and eyes-open resting conditions. Clinical Neurophysiology 118, 2765-2773.

Behzadi, Y., Restom, K., Liau, J., Liu, T.T., 2007. A component based noise correction method (CompCor) for BOLD and perfusion based fMRI. NeuroImage 37, 90-101.

Bianciardi, M., Fukunaga, M., van Gelderen, P., Horovitz, S.G., de Zwart, J.A., Duyn, J.H., 2009. Modulation of spontaneous fMRI activity in human visual cortex by behavioral state. NeuroImage 45, 160-168.

Birn, R.M., 2012. The role of physiological noise in resting-state functional connectivity. NeuroImage 62, 864-870.

Biswal, B., Yetkin, F.Z., Haughton, V.M., Hyde, J.S., 1995. Functional Connectivity in the Motor Cortex of Resting Human Brain Using Echo-Planar Mri. Magnetic Resonance in Medicine 34, 537-541.

Buxton, R.B., Uludag, K., Dubowitz, D.J., Liu, T.T., 2004. Modeling the hemodynamic response to brain activation. NeuroImage 23 Suppl 1, S220-233.

Caporro, M., Haneef, Z., Hsiang, J., Lenartowicz, A., Buttinelli, C., Parvizi, J., Stern, J.M., 2012. Functional MRI of sleep spindles and K-complexes. Clinical neurophysiology : official journal of the International Federation of Clinical Neurophysiology 123, 303-309.

Chang, C., Glover, G.H., 2009. Effects of model-based physiological noise correction on default mode network anti-correlations and correlations. NeuroImage 47, 1448-1459.

Cox, R.W., 1996. AFNI: software for analysis and visualization of functional magnetic resonance neuroimages. Comput Biomed Res 29, 162-173.

Debener, S., Strobel, A., Sorger, B., Peters, J., Kranczioch, C., Engel, A.K., Goebel, R., 2007. Improved quality of auditory event-related potentials recorded simultaneously with 3-T fMRI: removal of the ballistocardiogram artefact. NeuroImage 34, 587-597.

Delorme, A., Makeig, S., 2004. EEGLAB: an open source toolbox for analysis of single-trial EEG dynamics including independent component analysis. J Neurosci Methods 134, 9-21.

Devore, J.L., Farnum, N.R., 2005. Applied statistics for engineers and scientists, 2nd ed. Thomson Brooks/Cole, Belmont, CA.

Fox, M.D., Raichle, M.E., 2007. Spontaneous fluctuations in brain activity observed with functional magnetic resonance imaging. Nat Rev Neurosci 8, 700-711.

Fox, M.D., Snyder, A.Z., Vincent, J.L., Corbetta, M., Van Essen, D.C., Raichle, M.E., 2005. The human brain is intrinsically organized into dynamic, anticorrelated functional networks. Proceedings of the National Academy of Sciences of the United States of America 102, 9673-9678.

Fox, M.D., Zhang, D., Snyder, A.Z., Raichle, M.E., 2009. The global signal and observed anticorrelated resting state brain networks. J Neurophysiol 101, 3270-3283.

Fransson, P., 2005. Spontaneous low-frequency BOLD signal fluctuations: an fMRI investigation of the resting-state default mode of brain function hypothesis. Hum Brain Mapp 26, 15-29.

Fredholm, B.B., Battig, K., Holmen, J., Nehlig, A., Zvartau, E.E., 1999. Actions of caffeine in the brain with special reference to factors that contribute to its widespread use. Pharmacol Rev 51, 83-133.

Fukunaga, M., Horovitz, S.G., van Gelderen, P., de Zwart, J.A., Jansma, J.M., Ikonomidou, V.N., Chu, R., Deckers, R.H., Leopold, D.A., Duyn, J.H., 2006. Large-amplitude, spatially correlated fluctuations in BOLD fMRI signals during extended rest and early sleep stages. Magn Reson Imaging 24, 979-992.
Glover, G.H., Li, T.Q., Ress, D., 2000. Image-based method for retrospective correction of physiological motion effects in fMRI: RETROICOR. Magn Reson Med 44, 162-167.
Greicius, M.D., Krasnow, B., Reiss, A.L., Menon, V., 2003. Functional connectivity in the resting brain: a network analysis of the default mode hypothesis. Proc Natl Acad Sci U S A 100, 253-258.
Hahamy, A., Calhoun, V., Pearlson, G., Harel, M., Stern, N., Attar, F., Malach, R., Salomon, R., 2014. Save the global: global signal connectivity as a tool for studying clinical populations with functional magnetic resonance imaging. Brain Connect 4, 395-403.
Horovitz, S.G., Fukunaga, M., de Zwart, J.A., van Gelderen, P., Fulton, S.C., Balkin, T.J., Duyn, J.H., 2008. Low frequency BOLD fluctuations during resting wakefulness and light sleep: a simultaneous EEG-fMRI study. Hum Brain Mapp 29, 671-682.
Jahnke, K., von Wegner, F., Morzelewski, A., Borisov, S., Maischein, M., Steinmetz, H., Laufs, H., 2012. To wake or not to wake? The two-sided nature of the human K-complex. NeuroImage 59, 1631-1638.
Jansen, M., White, T.P., Mullinger, K.J., Liddle, E.B., Gowland, P.A., Francis, S.T., Bowtell, R., Liddle, P.F., 2012. Motion-related artefacts in EEG predict neuronally plausible patterns of activation in fMRI data. NeuroImage 59, 261-270.
Jao, T., Vertes, P.E., Alexander-Bloch, A.F., Tang, I.N., Yu, Y.C., Chen, J.H., Bullmore, E.T., 2013. Volitional eyes opening perturbs brain dynamics and functional connectivity regardless of light input. NeuroImage 69, 21-34.
Jobert, M., Schulz, H., Jahnig, P., Tismer, C., Bes, F., Escola, H., 1994. A computerized method for detecting episodes of wakefulness during sleep based on the alpha slow-wave index (ASI). Sleep 17, 37-46.
Larson-Prior, L.J., Zempel, J.M., Nolan, T.S., Prior, F.W., Snyder, A.Z., Raichle, M.E., 2009. Cortical network functional connectivity in the descent to sleep. Proc Natl Acad Sci U S A 106, 4489-4494.
Laufs, H., Daunizeau, J., Carmichael, D.W., Kleinschmidt, A., 2008. Recent advances in recording electrophysiological data simultaneously with magnetic resonance imaging. NeuroImage 40, 515-528.
Laurienti, P.J., Field, A.S., Burdette, J.H., Maldjian, J.A., Yen, Y.F., Moody, D.M., 2002. Dietary caffeine consumption modulates fMRI measures. NeuroImage 17, 751-757.
Liu, X., Yanagawa, T., Leopold, D.A., Chang, C., Ishida, H., Fujii, N., Duyn, J.H., 2015a. Arousal transitions in sleep, wakefulness, and anesthesia are characterized by an orderly sequence of cortical events. NeuroImage 116, 222-231.
Liu, X., Yanagawa, T., Leopold, D.A., Scholvink, M., Chang, C., Ishida, H., Fujii, N., Duyn, J.H., 2015b. Contribution of A Brain-state Specific Neurophysiological Event to Large-scale fMRI Signal Fluctuations. Annual Meeting of the International Society for Magnetic Resonance in Medicine, Toronto, p. 2107.
Matejcek, M., 1982. Vigilance and the EEG. In: Herrmann, W.M. (Ed.), Electroencephalography in drug research. Gustav Fischer, Stuttgart.
McAvoy, M., Larson-Prior, L., Nolan, T.S., Vaishnavi, S.N., Raichle, M.E., d'Avossa, G., 2008. Resting states affect spontaneous BOLD oscillations in sensory and paralimbic cortex. J Neurophysiol 100, 922-931.
Michels, L., Muthuraman, M., Luchinger, R., Martin, E., Anwar, A.R., Raethjen, J., Brandeis, D., Siniatchkin, M., 2013. Developmental changes of functional and directed resting-state connectivities associated with neuronal oscillations in EEG. NeuroImage 81, 231-242.
Muller, B., Gabelein, W.D., Schulz, H., 2006. A taxonomic analysis of sleep stages. Sleep 29, 967-974.
Murphy, K., Birn, R.M., Handwerker, D.A., Jones, T.B., Bandettini, P.A., 2009. The impact of global signal regression on resting state correlations: are anti-correlated networks introduced? NeuroImage 44, 893-905.

Neidermeyer, E., 1999. The Normal EEG of the Waking Adult. In: Neidermeyer, E., Lopes da Silva, F.H. (Eds.), Electroencephalography: basic principles, clinical applications and related fields. Lippincott Williams & Wilkins, Baltimore MD, pp. 149–173.
Niazy, R.K., Beckmann, C.F., Iannetti, G.D., Brady, J.M., Smith, S.M., 2005. Removal of FMRI environment artifacts from EEG data using optimal basis sets. NeuroImage 28, 720-737.
Olbrich, S., Mulert, C., Karch, S., Trenner, M., Leicht, G., Pogarell, O., Hegerl, U., 2009. EEG-vigilance and BOLD effect during simultaneous EEG/fMRI measurement. NeuroImage 45, 319-332.
Olbrich, S., Sander, C., Matschinger, H., Mergl, R., Trenner, M., Schönknecht, P., Hegerl, U., 2011. Brain and Body. Journal of Psychophysiology 25, 190-200.
Ong, J.L., Kong, D., Chia, T.T.Y., Tandi, J., Thomas Yeo, B.T., Chee, M.W.L., 2015. Co-activated yet disconnected-Neural correlates of eye closures when trying to stay awake. NeuroImage.
Patriat, R., Molloy, E.K., Meier, T.B., Kirk, G.R., Nair, V.A., Meyerand, M.E., Prabhakaran, V., Birn, R.M., 2013. The effect of resting condition on resting-state fMRI reliability and consistency: a comparison between resting with eyes open, closed, and fixated. NeuroImage 78, 463-473.
Power, J.D., Barnes, K.A., Snyder, A.Z., Schlaggar, B.L., Petersen, S.E., 2012. Spurious but systematic correlations in functional connectivity MRI networks arise from subject motion. NeuroImage 59, 2142-2154.
Raichle, M.E., MacLeod, A.M., Snyder, A.Z., Powers, W.J., Gusnard, D.A., Shulman, G.L., 2001. A default mode of brain function. Proc Natl Acad Sci U S A 98, 676-682.
Saad, Z.S., Gotts, S.J., Murphy, K., Chen, G., Jo, H.J., Martin, A., Cox, R.W., 2012. Trouble at rest: how correlation patterns and group differences become distorted after global signal regression. Brain Connect 2, 25-32.
Sadaghiani, S., Scheeringa, R., Lehongre, K., Morillon, B., Giraud, A.L., Kleinschmidt, A., 2010. Intrinsic connectivity networks, alpha oscillations, and tonic alertness: a simultaneous electroencephalography/functional magnetic resonance imaging study. J Neurosci 30, 10243-10250.
Scholvinck, M.L., Maier, A., Ye, F.Q., Duyn, J.H., Leopold, D.A., 2010. Neural basis of global resting-state fMRI activity. Proc Natl Acad Sci U S A 107, 10238-10243.
Smith, S.M., Jenkinson, M., Woolrich, M.W., Beckmann, C.F., Behrens, T.E., Johansen-Berg, H., Bannister, P.R., De Luca, M., Drobnjak, I., Flitney, D.E., Niazy, R.K., Saunders, J., Vickers, J., Zhang, Y., De Stefano, N., Brady, J.M., Matthews, P.M., 2004. Advances in functional and structural MR image analysis and implementation as FSL. NeuroImage 23 Suppl 1, S208-219.
Stern, J.M., Caporro, M., Haneef, Z., Yeh, H.J., Buttinelli, C., Lenartowicz, A., Mumford, J.A., Parvizi, J., Poldrack, R.A., 2011. Functional imaging of sleep vertex sharp transients. Clin Neurophysiol 122, 1382-1386.
Tagliazucchi, E., Laufs, H., 2014. Decoding wakefulness levels from typical fMRI resting-state data reveals reliable drifts between wakefulness and sleep. Neuron 82, 695-708.
Tagliazucchi, E., von Wegner, F., Morzelewski, A., Brodbeck, V., Jahnke, K., Laufs, H., 2013. Breakdown of long-range temporal dependence in default mode and attention networks during deep sleep. Proc Natl Acad Sci U S A 110, 15419-15424.
Viola, F.C., Thorne, J., Edmonds, B., Schneider, T., Eichele, T., Debener, S., 2009. Semi-automatic identification of independent components representing EEG artifact. Clin Neurophysiol 120, 868-877.
Wong, C.W., Olafsson, V., Tal, O., Liu, T.T., 2012. Anti-correlated networks, global signal regression, and the effects of caffeine in resting-state functional MRI. NeuroImage 63, 356-364.
Wong, C.W., Olafsson, V., Tal, O., Liu, T.T., 2013. The amplitude of the resting-state fMRI global signal is related to EEG vigilance measures. NeuroImage 83, 983-990.
Woolrich, M.W., Jbabdi, S., Patenaude, B., Chappell, M., Makni, S., Behrens, T., Beckmann, C., Jenkinson, M., Smith, S.M., 2009. Bayesian analysis of neuroimaging data in FSL. NeuroImage 45, S173-186.

Xu, P., Huang, R., Wang, J., Van Dam, N.T., Xie, T., Dong, Z., Chen, C., Gu, R., Zang, Y.F., He, Y., Fan, J., Luo, Y.J., 2014. Different topological organization of human brain functional networks with eyes open versus eyes closed. NeuroImage 90, 246-255.
Yan, C.G., Liu, D.Q., He, Y., Zou, Q.H., Zhu, C.Z., Zuo, X.N., Long, X.Y., Zang, Y.F., 2009. Spontaneous Brain Activity in the Default Mode Network Is Sensitive to Different Resting-State Conditions with Limited Cognitive Load. PLoS One 4, e5743.
Yang, G.J., Murray, J.D., Repovs, G., Cole, M.W., Savic, A., Glasser, M.F., Pittenger, C., Krystal, J.H., Wang, X.J., Pearlson, G.D., Glahn, D.C., Anticevic, A., 2014. Altered global brain signal in schizophrenia. Proc Natl Acad Sci U S A 111, 7438-7443.
Yang, H., Long, X.Y., Yang, Y.H., Yan, H., Zhu, C.Z., Zhou, X.P., Zang, Y.F., Gong, Q.Y., 2007. Amplitude of low frequency fluctuation within visual areas revealed by resting-state functional MRI. NeuroImage 36, 144-152.
Yeo, B.T.T., Tandi, J., Chee, M.W.L., 2015. Functional connectivity during rested wakefulness predicts vulnerability to sleep deprivation. NeuroImage 111, 147-158.
Yuan, B.K., Wang, J., Zang, Y.F., Liu, D.Q., 2014. Amplitude differences in high-frequency fMRI signals between eyes open and eyes closed resting states. Front Hum Neurosci 8, 503.
Zou, Q.H., Long, X.Y., Zuo, X.N., Yan, C.G., Zhu, C.Z., Yang, Y.H., Liu, D.Q., He, Y., Zang, Y.F., 2009. Functional Connectivity Between the Thalamus and Visual Cortex Under Eyes Closed and Eyes Open Conditions: A Resting-State fMRI Study. Human Brain Mapping 30, 3066-3078.

Figure 1

Click here to download high resolution image

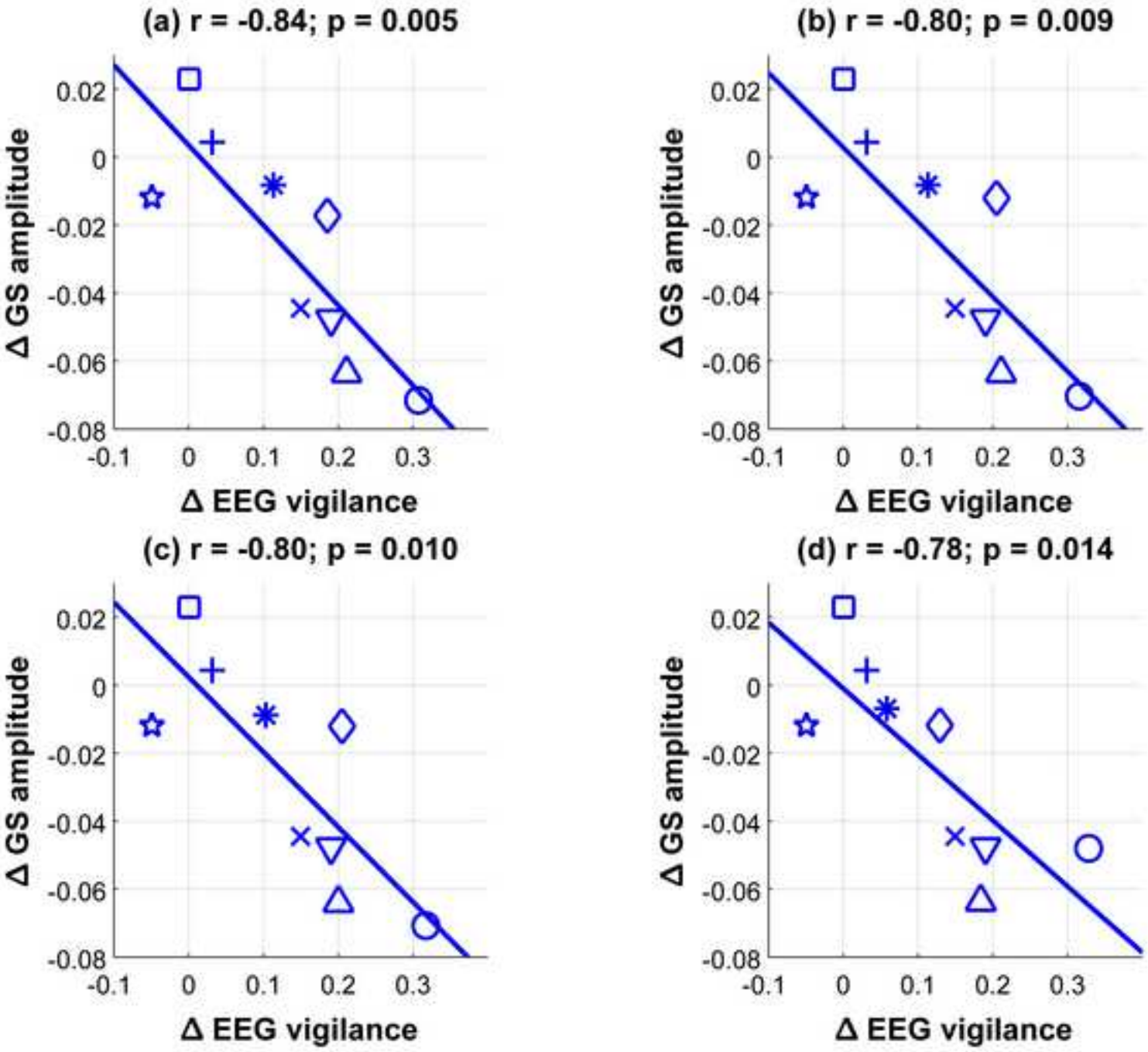

Figure 2

Click here to download high resolution image

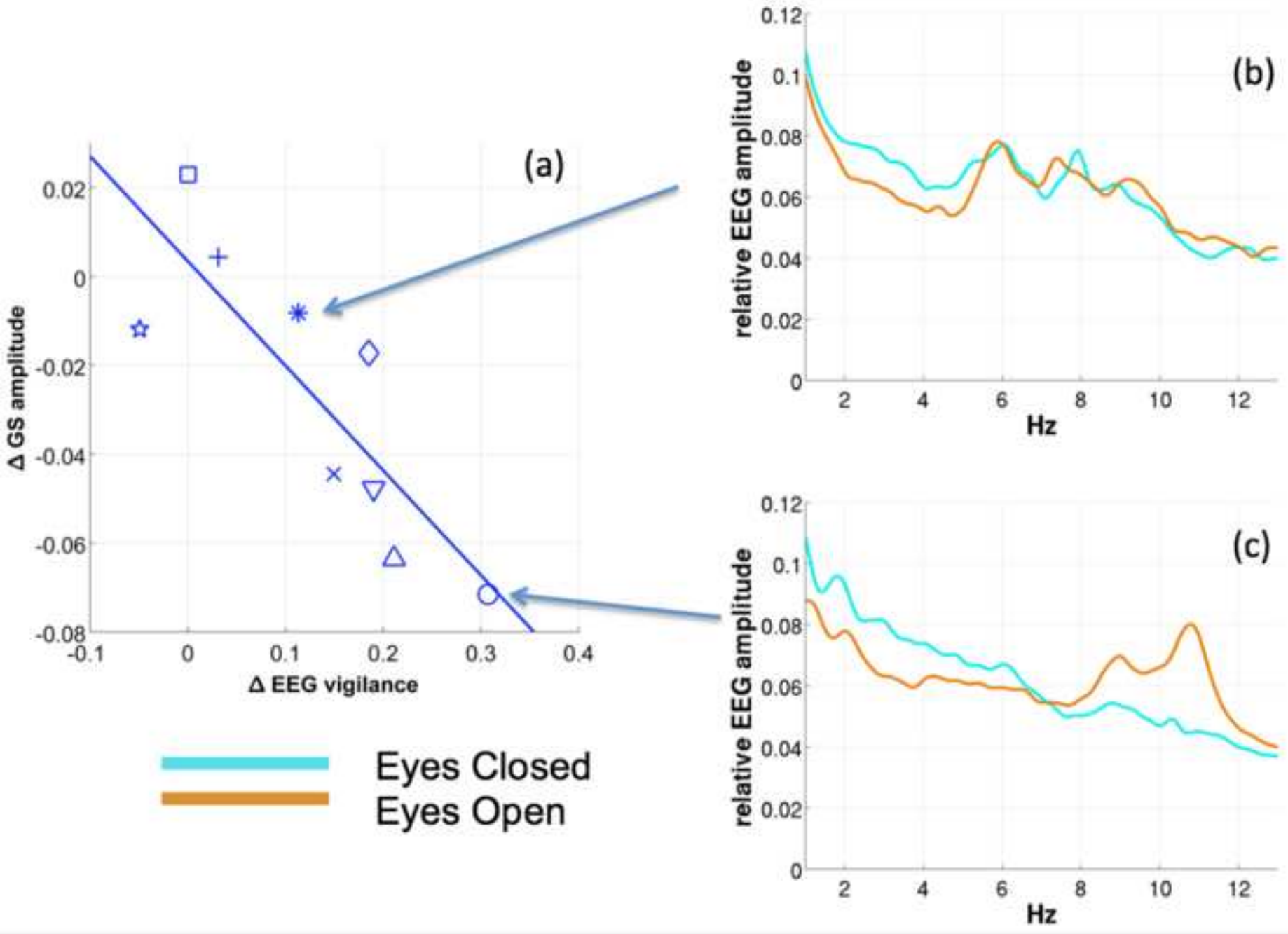

Figure 3

Click here to download high resolution image